Journal of Pediatric Surgery 59 (2024) 1549–1555

Contents lists available at ScienceDirect

Journal of Pediatric Surgery

journal homepage: www.sciencedirect.com/journal/journal-of-pediatric-surgery

Clinical Application and Further Development of Augmented Reality Guidance for the Surgical Localization of Pediatric Chest Wall Tumors

Rémi van der Woude [a, b], Matthijs Fitski [a], Jasper M. van der Zee [a, b], Cornelis P. van de Ven [a], Guus M.J. Bökkerink [a], Marc H.W.A. Wijnen [a], Jene W. Meulstee [c], Tristan P.C. van Doormaal [c, d], Françoise J. Siepel [e], Alida F.W. van der Steeg [a, *]

[a] Princess Máxima Center for Pediatric Oncology, Heidelberglaan 25, 3584 CS, Utrecht, the Netherlands
[b] Technical Medicine, TechMed Centre, University of Twente, Drienerlolaan 5, 7522 NB, Enschede, the Netherlands
[c] Augmedit B.V., Naarden, the Netherlands
[d] Department of Neurosurgery, Brain Division, University Medical Center, Utrecht, the Netherlands
[e] Robotics and Mechatronics, TechMed Centre, University of Twente, Drienerlolaan 5, 7522 NB, Enschede, the Netherlands

ARTICLE INFO

Article history:
Received 13 February 2024
Accepted 16 February 2024

Keywords:
Augmented reality
Chest wall resections
Tumor localization
Point-based registration
Surface matching

ABSTRACT

Background: Surgical treatment of pediatric chest wall tumors requires accurate surgical planning and tumor localization to achieve radical resections while sparing as much healthy tissue as possible. Augmented Reality (AR) could facilitate surgical decision making by improving anatomical understanding and intraoperative tumor localization.
We present our clinical experience with the use of an AR system for intraoperative tumor localization during chest wall resections. Furthermore, we present the pre-clinical results of a new registration method to improve our conventional AR system.
Methods: From January 2021, we used the HoloLens 2 for pre-incisional tumor localization during all chest wall resections inside our center. A patient-specific 3D model was projected onto the patient by use of a five-point registration method based on anatomical landmarks. Furthermore, we developed and pre-clinically tested a surface matching method to allow post-incisional AR guidance by performing registration on the exposed surface of the ribs.
Results: Successful registration and holographic overlay were achieved in eight patients. The projection seemed most accurate when landmarks were positioned in a non-symmetric configuration in proximity to the tumor. Disagreements between the overlay and expected tumor location were mainly due to user-dependent registration errors. The pre-clinical tests of the surface matching method proved the feasibility of registration on the exposed ribs.
Conclusions: Our results prove the applicability of AR guidance for the pre- and post-incisional localization of pediatric chest wall tumors during surgery. The system has the potential to enable intraoperative 3D visualization, hereby facilitating surgical planning and management of chest wall resections.
Level of Evidence: IV
Type of Study: Treatment Study

1. Introduction

Pediatric chest wall tumors represent a heterogeneous group of malignancies. The most frequent is the Ewing sarcoma, followed by a spectrum of other sarcomas such as rhabdomyosarcoma, osteosarcoma, and chondrosarcoma [1]. Due to the aggressive nature of these chest wall tumors, the primary surgical goal is complete tumor removal with a wide margin [2–5]. However, the inevitable

Abbreviations: AR, Augmented Reality; CT, Computed tomography; HMD, Head-Mounted Display; ioMRI, Intraoperative Magnetic Resonance Imaging; ioUS, Intraoperative Ultrasound; ICP, Iterative Closest Point; OR, Operation Room; QR, Quick Response; RMS, Root Mean Square; TRE, Target Registration Error; 3D, Three-Dimensional; 2D, Two-Dimensional.

* Corresponding author. Heidelberglaan 25, 3584 CS Utrecht, the Netherlands.
E-mail address: A.F.W.vanderSteeg@prinsesmaximacentrum.nl (A.F.W. van der Steeg).

https://doi.org/10.1016/j.jpedsurg.2024.02.023

removal of multiple ribs can lead to significant chest wall deformities that impact respiration, mobilization and aesthetics [4,6]. To balance radical resection and preserving healthy tissue, precise surgical planning and adequate tumor localization are crucial. However, the intraoperative localization of chest wall tumors, e.g. Ewing sarcoma, can be extremely difficult. These tumors often grow inward and are therefore invisible from the outside. Additionally, they have often shrunk enormously and become non-palpable after neo-adjuvant chemotherapy [7,8]. Currently, intraoperative localization of the affected rib leads to a very complex and time-consuming procedure based on multiple two-dimensional (2D) imaging modalities, palpation and thoracoscopy [7]. Subsequently, the length and result of this procedure still heavily relies on the surgeon's spatial interpretation which can lead to variations in outcome.

The use of intraoperative guidance could overcome these challenges by facilitating better and faster intraoperative tumor localization. Hereby Augmented Reality (AR) has the advantage of being a non-invasive visualization technique that can give a direct impression of the patient's anatomy in 3D. When used with a head-mounted display (HMD), such as the HoloLens 2 (Microsoft Corporation, Redmond, WA, USA), patient-specific 3D segmentations based on preoperative imaging can be projected directly onto the patient in the working field of the surgeon. This enables a more intuitive interpretation of the patient's anatomy and circumvents the need for additional and invasive imaging modalities [9–13]. However, these projections are notoriously inaccurate. Therefore, to facilitate an accurate match between the hologram and the patient a method of registration is needed.

Our group previously described the first use of AR to guide a chest wall resection in a pediatric patient in 2022 [14] using a point-based registration with anatomical landmarks on the skin. In the current paper we present our clinical experience with its use in 8 subsequent pediatric chest wall resections. A drawback of this method is the limited possibility to further use the AR system during the intraoperative phase, because hereto re-registration is often needed. This is not possible using the point-based method because of deformation and shifting of the skin once the first incision has been made.

An alternative way of registration is surface matching. Surface matching registration methods find the most optimal transformation between two large sets of points, i.e. point clouds, that make up a surface [15,16]. Within surgical applications, surface matching can be performed on surfaces of anatomical structures, for example the surface of the skin, an organ or bone [17–19]. Surface matching methods do not depend on the selection of anatomical landmarks and can therefore still be performed once the skin has been opened. Additionally, the algorithms that are generally used for surface matching do not require the two corresponding point clouds to consist of the same number of points. This means that registration can be performed on only a limited exposed part of the total surface, and therefore facilitates intraoperative registration [20]. We have investigated the feasibility of surface matching to allow registration on the post-incisional surgical field, i.e. the exposed surface of the ribs. We therefore implemented surface matching into our AR system, and hereby present its first preclinical results.

2. Material and methods

2.1. Point-based registration in patients

From the first of January 2021 to June 2023 a total of eight subsequent patients underwent surgical resection of a chest wall tumor in the Princess Máxima Center (Utrecht, The Netherlands) with the use of AR. For all 8 patients, a patient-specific 3D model was created by manual segmentation of the tumor and relevant anatomy from preoperative computed tomography (CT) images (Version 5.0.3, The Slicer Community, http://www.slicer.org [21]). There were no safety margins included in this model as our primary objective was to locate the tumor correctly. Subsequently, the model was projected onto the patient in the operation room (OR) by use of a five-point registration method based on anatomical landmarks.

2.1.1. 3D model preparation

The first step in the preoperative registration workflow is the selection of anatomical landmarks during the preoperative CT scan, which is performed approximately two weeks prior to surgery and standard of care in our center. During this scan, all patients were positioned in the surgical lateral decubitus position to prevent possible registration inaccuracies caused by deformations of the thorax between the preoperative CT scan and intraoperative situation. Subsequently, a minimum of five recognizable points was selected on the skin as registration landmarks (Fig. 1A). Radiopaque Lead-Balls (Suremark®, Mesa, AZ, USA) were attached to structures such as the nipple, birthmarks, or scars. If too few recognizable points could be distinguished, a skin marker was used to manually draw the remaining landmarks on the chest. Together with the tumor and relevant anatomical structures, the Lead-Balls were segmented from the preoperative CT scan to digitally indicate the positions of these anatomical landmarks inside the 3D model (Fig. 1B). All segmentations were performed by technical physicians specifically trained in Ewing sarcoma delineation and controlled and approved by the performing surgeon (CvdV). Finally, the 3D model and anatomical landmarks were transferred to Unity (Version 2019.4.39f1, Unity Technologies, San Francisco, CA, USA) where the HoloLens 2 application was built. This process of preparation of the 3D model, control, approval and transfer to Unity takes 1–3 days in total.

2.1.2. Point-based registration

The landmark point-based registration enables a holographic overlay of the 3D model onto the patient in the OR by matching the digital positions of the landmarks with the intraoperative positions of the corresponding landmarks on the patient's skin. During registration, a reference quick response (QR) code was attached to the patient's lower ribs, hip, or shoulder. This facilitated continuous tracking and position correction of the hologram (for example during bed movement). Subsequently, the surgeon indicated each sequential anatomical landmark on the patient's skin with a 3D printed pointer in which another QR code was included and saved its position relative to the attached QR code using a voice command (Fig. 1C). When all five points were registered, a Procrustes algorithm computed the most optimal transformation matrix to correctly align the virtual 3D model with the patient in the OR (Fig. 1D). The surgeons qualitatively interpreted projection accuracy by visually comparing the hologram placement to the tumor localization based on manual palpation and thoracoscopy.

2.2. Surface matching for intraoperative registration

Based on the clinical need to further use the AR system during the intraoperative phase, we developed a surface matching AR system to perform registration on the post-incisional surface of the exposed ribs. First, a phantom study was performed to determine the registration time and projection accuracy. Subsequently, a human cadaver study was performed to explore the feasibility of surface matching in a surgical setting.

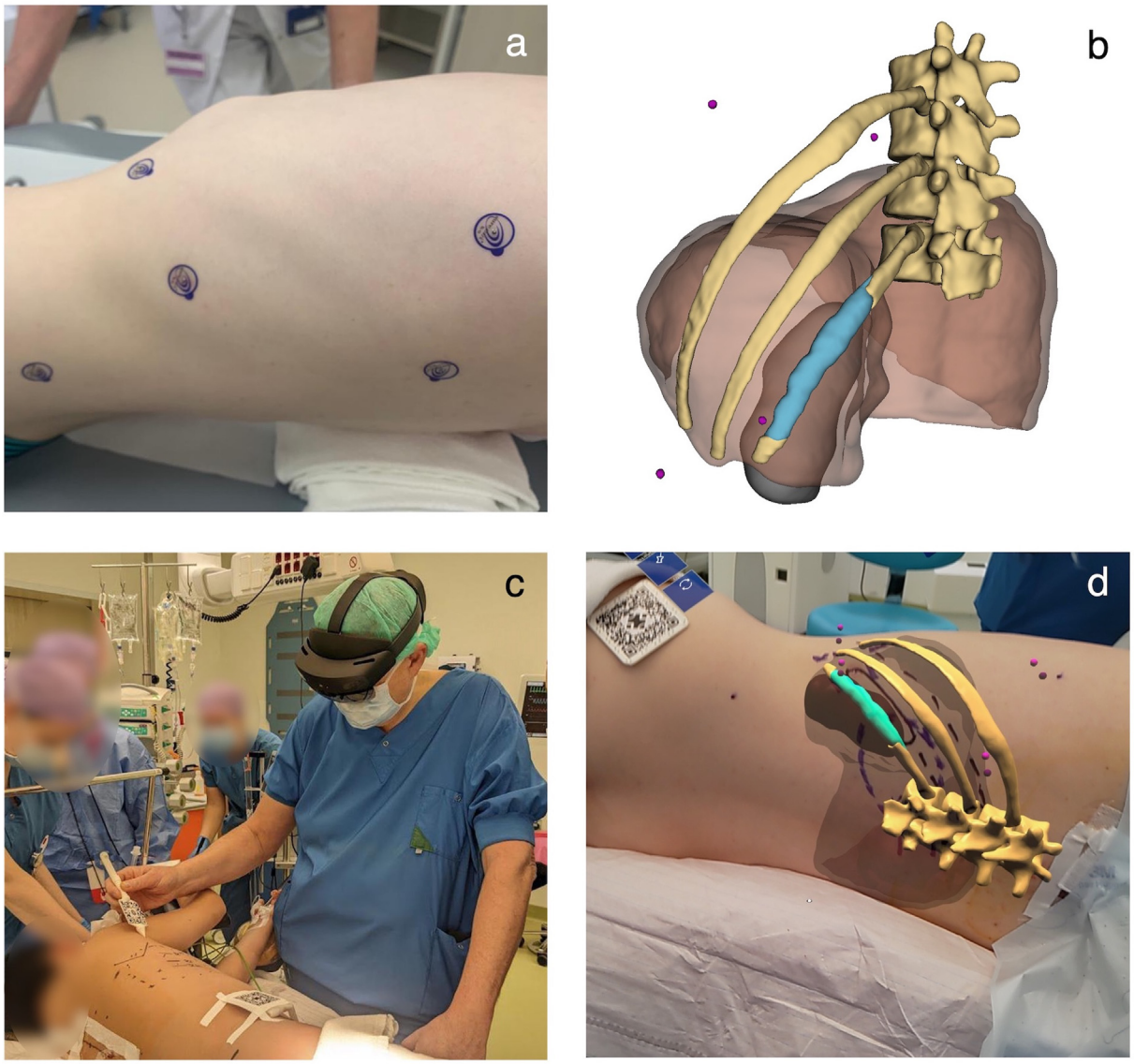

Fig. 1. Landmark point-based registration workflow. (A) Selection of anatomical landmarks with the patient lying in lateral decubitus position during preoperative CT scan. (B) Virtual 3D model of ribs, tumor (blue), landmarks (purple spheres) and relevant anatomy (diaphragm and kidney). (C) Surgeon performing landmark point-based registration with the 3D printed pointer. The reference QR code is attached to the patient's hip. (D) Projection of the virtual model onto the patient. Note that there can be an apparent misalignment in these figures between the patient and holographic overlay due to the displacement between the HoloLens camera and the surgeon's line of sight.

2.2.1. Technical background surface matching system

A demonstration of our surface matching system on a 3D printed phantom is shown in Fig. 2. During registration, a preoperative point cloud of the post-incision surgical field is matched to the corresponding intraoperative surface. The preoperative point cloud was derived from CT images by manual segmentation and reconstruction of the intercostal muscles and contour of the relevant ribs, to mimic the surgical field. Subsequently, the corresponding intraoperative surface point cloud was acquired by tracing the surgical pointer with QR code along the contour of the exposed ribs (Fig. 2A). Hereto, after a voice command in a dedicated application (Augmedit B.V., Naarden, The Netherlands), the HoloLens continuously tracked the surgical pointer and saved the 3D position of the tip every 0.5 s. Consequently, by tracing the pointer across the exposed surgical field, eventually a point cloud is acquired of the post-incision surface (Fig. 2B). When the whole surface was covered, the voice command “Stop” ended the point cloud acquisition. Subsequently, the transformation matrix between the pre- and intraoperative point clouds was computed with an iterative closest point (ICP) algorithm run on an external Python server (Augmedit B.V., Naarden, The Netherlands). This transformation matrix was then sent back to the HoloLens application to correctly project the 3D model onto the post-incision surface.

2.2.2. Phantom study

We measured the target registration error (TRE) and registration time of the surface matching system on a 3D printed phantom of a 10-year-old child. The phantom study was performed by two observers, both an experienced and unexperienced HoloLens user. Per observer, registration was timed and repeated five times. After each registration was completed, nine target points were projected onto the phantom. The user was instructed to objectively mark the positions of each target with a pencil, while keeping their head as still as possible to eliminate the effect of drift. A digital caliper with 0.01 mm accuracy was

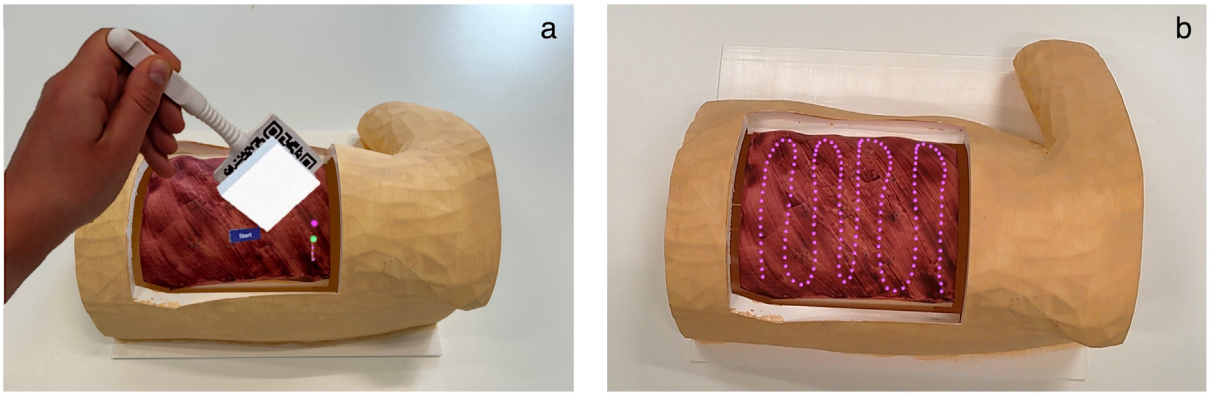

Fig. 2. Example of the surface matching system on the post-incision surface of a 3D printed phantom. (A) Point cloud acquisition by tracing the surgical pointer with QR code across the post-incisional surface. (B) Total acquired point cloud used for registration.

used to measure the 2D distance between the marked points and five beacon points included in the post-incision surface of the phantom. Using these measurements, the 3D position of the marked points was computed in Python with the use of a trilateration principle [22]. The TRE was computed as the Root Mean Square error (RMS), or Euclidian distance, between the 3D positions of the marked targets and the 3D positions of the virtual targets. Finally, student T-tests were performed to analyze inter-observer variability in TRE values and registration times.

2.2.3. Cadaver study

The main goal of the cadaver study was to investigate whether surgeons were able to locate the correct rib with use of post-incisional surface matching. Therefore, two pediatric oncologic surgeons performed a chest wall resection on a human thorax with use of AR guidance. First, a virtual 3D model of three ribs and an imaginary tumor was created based on preoperative CT images of the frozen cadavers. Subsequently, after performing registration on the exposed ribs of the thawed cadavers, the surgeons had to mark the edges of the imaginary tumor with a surgical saw based on palpation, their own interpretation of the anatomy and holographic overlay of the virtual 3D model. Finally, another CT scan was made to reconstruct a postoperative 3D model of the three ribs and marked tumor edges. This model was registered to the preoperative virtual model (CloudCompare, Version 2.12.3, Open GL, R&D EDF) to evaluate whether surgeons located the correct rib and to qualitatively assess the accuracy of the resection.

3. Results

3.1. Point-based registration in patients

Technical successful registration was achieved in all eight patients (Table 1).

Figure 3 shows two examples of the pre-incisional visualization of the 3D model after point-based registration. Note that there can be an apparent misalignment in these figures between the patient and holographic overlay due to the displacement between the HoloLens camera and the surgeon's line of sight. When qualitatively interpreting the projection accuracy based on the comparison with palpation and thoracoscopy, surgeons indicated that the projection of the 3D model was sufficiently accurate to locate the affected rib in most patients. In some cases, registration inaccuracies resulted in disagreements between the overlay and expected tumor location based on palpation or thoracoscopy. Regardless of the holographic overlay, resection was always performed based on the conventional imaging techniques.

3.2. Phantom study

Per observer, nine target measurements were performed five times, resulting in a total of 90 TRE measurements (Table 2). The phantom study showed that users were able to locate targets with an accuracy of 6.2 ± 5.0 mm with registration times of 51 ± 6 s on average. The average standard deviations were calculated based on the standard deviation of each registration moment (e.g. five per observer). Statistical analysis showed a significant difference between the TRE values of both observers ($p < 0.001$). There was no significant difference between the registration times for each observer.

3.3. Cadaver study

Both surgeons were able to achieve a successful holographic overlay after performing registration on the exposed ribs (Fig. 4A). Reconstruction of the postoperative CT scan showed that both surgeons located the tumor in the correct rib with high precision, though it was difficult to quantify the exact accuracy of resection

Table 1
Patient characteristics.

Patient	Sex	Age (y)	Tumor	Resected ribs	Neoadjuvant chemotherapy	Tumor measurement at diagnosis (AP x RL x CC) (cm)	Preoperative tumor measurement (AP x RL x CC) (cm)
1	F	6	Ewing sarcoma	7th	Yes	11.2 x 14.9 x 19.9 (3321 ml)	4.6 x 2.5 x 5.9 (68 ml)
2	M	12	Ewing sarcoma	8th - 10th	Yes	5.9 x 5.4 x 7.4 (236 ml)	5.8 x 1.3 x 4.5 (34 ml)
3	M	7	Ewing sarcoma	8th - 10th	Yes	4.6 x 6.4 x 5.6 (165 ml)	4.4 x 3.3 x 1.6 (23 ml)
4	M	2	Ewing sarcoma	7th	Yes	5.0 x 3.0 x 5.0 (75 ml)	2.6 x 1,8 x 1.1 (5 ml)
5	M	13	Mesenchymal chondrosarcoma	5th – 7th	No	9.1 x 7.1 x 7.6 (491 ml)	9.1 x 7.1 x 7.6 (491 ml)
6	M	10	Ewing sarcoma	6th – 8th	Yes	11.4 x 4.7 x 4.6 (246 ml)	10.0 x 3.6 x 2.1 (76 ml)
7	M		Ewing sarcoma	10th – 12th	Yes	9.9 x 8.0 x 13.4 (1061 ml)	6.2 x 2.0 x 7.8 (97 ml)
8	M	11	Ewing sarcoma	8th – 10th	Yes	3.0 x 2.0 x 4.2 (25 ml)	0.8 x 0.7 x 1.0 (1 ml)

Fig. 3. Two examples of the pre-incisional projection of the 3D model during surgery. The model includes the tumor, ribs, relevant anatomy, and registration landmarks (purple spheres). Note that there can be an apparent misalignment in these figures between patient and hologram due to the displacement between the HoloLens camera and the surgeon's line of sight.

due to tissue deformations between the pre- and postoperative CT scan (Fig. 4C). Overall, the surgeons were satisfied with the registration results and reported that the post-incision holographic overlay improved their confidence in localization of the correct rib and tumor.

4. Discussion

We first described our clinical experience with an AR system to localize chest wall tumors prior to incision. The conventional landmark point-based registration method seemed successful in most patients and was sufficiently accurate to locate the correct rib. Registration appeared most robust and accurate when the landmarks had a non-symmetric configuration in proximity to the tumor, as is supported by literature [23]. However, surgeons were only able to give a qualitative assessment of this projection accuracy, as it often remained uncertain whether the intraoperative tumor localization based on palpation or thoracoscopy was correct. Apparent misalignments between the holographic overlay and expected tumor localization based on palpation or thoracoscopy were mainly due to insufficient tracking of the reference QR code or user-dependent errors during registration, e.g. selecting incorrect birthmarks or scars, or not being able to recognize landmarks due to the use of (colored) disinfectant. Overall, surgeons were satisfied with the results and agreed on the potential of this system for the pre-incisional tumor localization during chest wall resections. Moreover, they expressed the clinical need for intraoperative AR guidance. The newly developed surface matching method seems to provide the basis for this technique by allowing post-incisional registration on the exposed ribs with sufficient accuracy.

The results of our clinical experiences and pre-clinical testing confirm the potential of AR to serve as a quick and non-invasive visualization technique during chest wall resections. Other alternatives that could be used for intraoperative tumor localization are intraoperative MRI (ioMRI) or (navigated) ultrasound (ioUS). These imaging modalities have the advantage of providing the true intraoperative situation of relevant anatomy. With ioMRI, the tumor and affected ribs could be located with high precision, but the procedure would have to be interrupted for a considerable amount of time. Navigated ioUS is a quicker imaging technique, but has a high interobserver variability and imaging quality of bony structures is not always sufficient. Additionally, both imaging techniques do not give a direct vision of exposed structures and still rely on the spatial interpretation of the operating surgeon. Consequently, AR seems the most preferred method for intraoperative tumor localization, though ioMRI or ioUS could serve as suitable imaging modalities to validate and quantify our systems accuracy in the future.

Table 2
Results of the Target Registration Error and registration times of surface matching on a 3D printed phantom.

	TRE ± std (mm)	Time ± std (s)
Observer 1	4.9 ± 2.2	51 ± 5
Observer 2	7.4 ± 1.4	51 ± 7
Mean	6.2 ± 5.0	51 ± 6

To our knowledge, this is the first clinical study to explore the use of AR within pediatric chest wall resections. Other AR system applications described are mainly in orthopedic, plastic, and maxillofacial surgery [24]. For example, Pratt et al. [25] demonstrated the use of the HoloLens for the mapping of perforating vessels during reconstructive surgery. They clinically implemented an AR system to project 3D vascular models onto the lower extremities to assist in identification, dissection, and execution of vascular pedunculated flaps. Yang et al. [26] describe AR in maxillofacial surgery. They used a similar landmark point-based registration method to project a virtual 3D planning onto the patient in the OR during mandible reconstructions. Both studies conclude that the use of an HMD, such as the HoloLens, improved anatomical understanding, operation times and surgical decision making. Furthermore, the use of the HoloLens allowed surgeons to limit their focus on the operation field, instead of switching between 2D monitors where the virtual models are generally displayed and the patient (the so-called switching focus problem). Our work supports these findings in literature and confirm the further applicability of AR, also within the field of pediatric surgical oncology.

When considering our surface matching method, a comparable cadaver study was performed by Hoch et al. [27] They used a similar registration method to perform a periacetabular osteotomy of Ganz with AR guidance. An orthopedic surgeon performed surface matching on the exposed pelvic bone and was able to achieve osteotomies with an accuracy of 6.6 mm based on the holographic overlay of a preoperative planning. As our cadaver experiments had a different set-up where surgeons performed the resection based on their own interpretation, it is difficult to directly compare the accuracy results of Hoch et al. with our cadaver study. However, it is expected that our surface matching method should be able to achieve comparable accuracy results when measuring TRE's values in a similar cadaver experiment.

Although the first experiences with the use of AR during chest wall resections seem promising, there are still several limitations

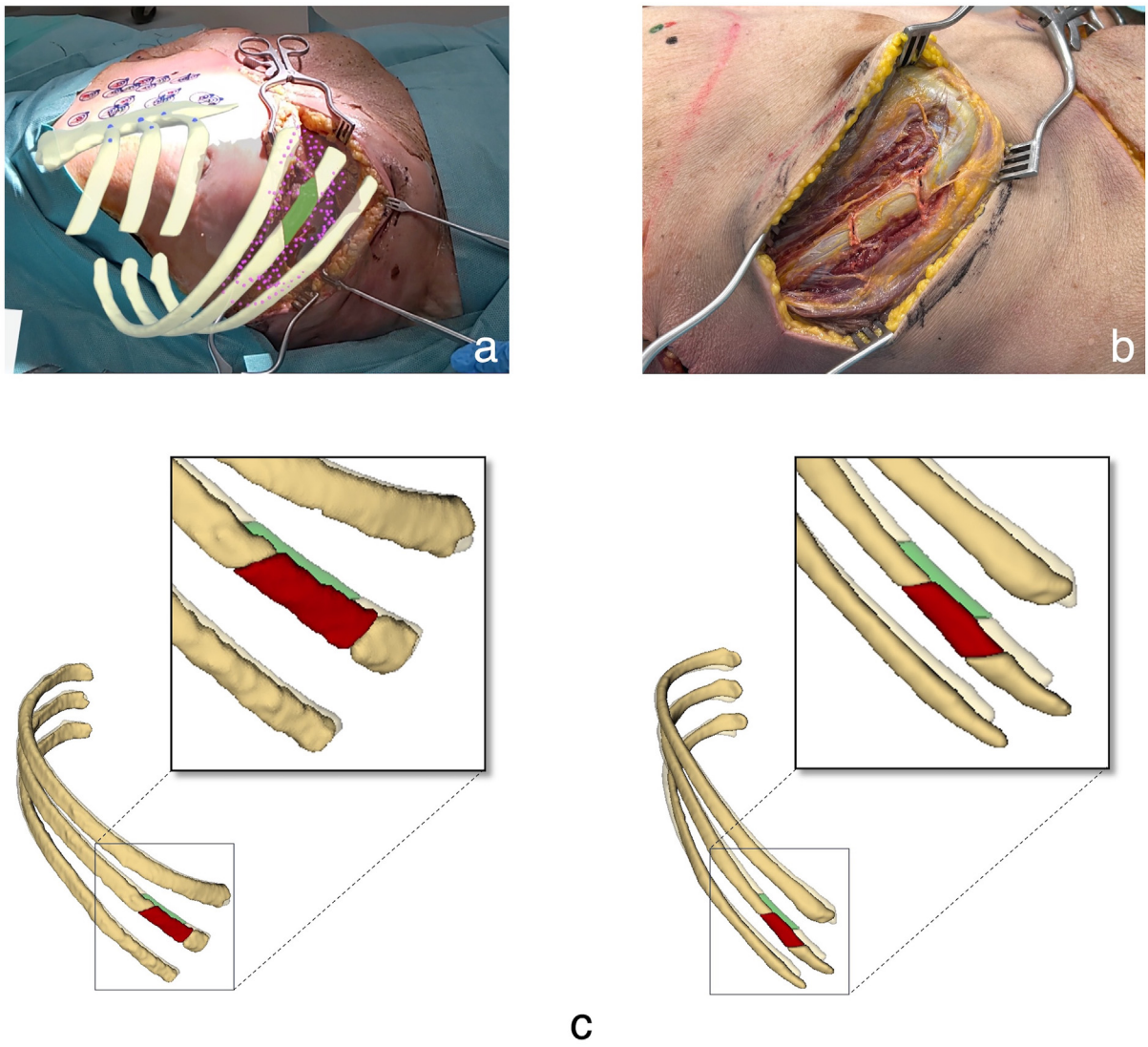

Fig. 4. Results of the cadaver experiment. (A) Holographic projection of ribs and imaginary tumor (green) after surface matching on the exposed ribs. The collection of pink spheres shows the intraoperative point cloud acquired by tracing the pointer across the post-incision surface. (B) Marking of the tumor edges with a surgical saw. (C) Resection results of both surgeons. The results show the reconstruction of the ribs and marked tumor (red) from postoperative CT scan together with the preoperative virtual model (transparent, tumor in green). Misalignments of the models can be due to segmentation differences, registration inaccuracies or tissue deformations between the scans.

that should be considered. First, the landmark point-based registration method was still prone to user-dependent errors and registration inaccuracies. Future efforts should be made to quantify and eliminate these potential errors to increase registration performance by improving the user-friendliness of the HoloLens application, exploring different registration techniques, and improving the surgeons' overall experience with the HoloLens. Second, the accuracy of our conventional AR system was only subjectively quantified by interpretation of the operating surgeons. Before this system can be used for actual surgical decision making and additional intraoperative imaging techniques can be left out, the exact registration accuracy should be thoroughly validated in clinical setting. The same accounts for the implementation of the surface matching method. The cadaver study solely proved the feasibility of post-incisional registration on the exposed surface of the ribs. Future experiments should focus on testing the surface matching method in an even more realistic setting to explore its actual registration accuracy, for example with tests on smaller cadavers or cadavers lying in lateral decubitus position. A last limitation is that our current registration methods are based on rigid transformations, which require the patient to lie in the same position during the preoperative CT scan as during surgery. This can be uncomfortable for the patient, but also easily induces registration inaccuracies as slight differences in this patient position are inevitable. In the future, registration algorithms based on elastic transformations could be explored, as these do not require the same patient position between the preoperative and intraoperative situation.

In conclusion, we presented our clinical experiences with an AR system to intraoperatively localize chest wall tumors prior to incision. Furthermore, we explored the use of a new surface matching method to allow additional AR guidance once the skin has been opened. Combining these results, our system has the potential to facilitate intraoperative tumor localization and surgical decision-making during chest wall resections. Future studies should focus on the validation of registration accuracies and the elimination of potential registration errors.

Financial support statement

This work was supported in-kind by the Princess Máxima Center for Pediatric Oncology. The research did not receive any specific grant from funding agencies in the public, commercial, or not-for-profit sectors. Augmedic B.V. (Naarden, The Netherlands) contributed in-kind to this work with software programming.

Conflicts of interest

Jene Meulstee is product owner of Augmedit. Tristan van Doormaal is Chief Medical Officer of Augmedit. Augmedit is a software company aimed at creating AI powered holographic operative support for surgeons.

Acknowledgments

The authors would like to thank Koen Spijkerboer and the 3D Lab of RadboudUMC (Nijmegen, The Netherlands) for the initial development of the landmark point-based registration method. Furthermore, the authors would like to thank Milan Wijnmaalen and the Augmedit team for the development of the surface matching method and their technical support.

References

[1] Shochat SJ, Sandoval JA. Chest wall tumors. In: Puri P, editor. Pediatric surgery: general pediatric surgery, tumors, trauma and transplantation. Berlin, Heidelberg: Springer; 2021. p. 1015–29. https://doi.org/10.1007/978-3-662-43559-5_155.
[2] Zöllner SK, Amatruda JF, Bauer S, et al. Ewing sarcoma—diagnosis, treatment, clinical challenges and future perspectives. J Clin Med 2021;10:1685. https://doi.org/10.3390/jcm10081685.
[3] EURO EWING Study Group. EWING 2008 protocol. 2018.
[4] Lopez C, Correa A, Vaporciyan A, et al. Outcomes of chest wall resections in pediatric sarcoma patients. J Pediatr Surg 2017;52:109–14. https://doi.org/10.1016/j.jpedsurg.2016.10.035.
[5] Bosma SE, van der Heijden L, Sierrasesúmaga L, et al. What do we know about survival in skeletally premature children aged 0 to 10 Years with ewing sarcoma? A multicenter 10-year follow-up study in 60 patients. Cancers 2022;14:1456. https://doi.org/10.3390/CANCERS14061456.
[6] Glotzbecker MP, Gold M, Puder M, et al. Scoliosis after chest wall resection. J Child Orthop 2013;7:301–7. https://doi.org/10.1007/S11832-013-0519-2/ASSET/IMAGES/LARGE/10.1007_S11832-013-0519-2-FIG2 [JPEG].
[7] Lelkes VM, Jones KB, Groundland JS. Chest wall resection for sarcoma: a surgical technique and case series. Operat Tech Orthop 2020;30:100801. https://doi.org/10.1016/j.oto.2020.100801.
[8] Basharkhah A, Lackner H, Karastaneva A, et al. Interdisciplinary radical "en-bloc" resection of ewing sarcoma of the chest wall and simultaneous chest wall repair achieves excellent long-term survival in children and adolescents. Frontiers in Pediatrics 2021;9:197. https://doi.org/10.3389/FPED.2021.661025/BIBTEX.
[9] Meulstee JW, Nijsink J, Schreurs R, et al. Toward holographic-guided surgery. Surg Innovat 2019;26:86–94. https://doi.org/10.1177/1553350618799552.
[10] Yoon JW, Chen RE, Kim EJ, et al. Augmented reality for the surgeon: systematic review. Int J Med Robot Comput Assist Surg 2018;14:1–13. https://doi.org/10.1002/rcs.1914.
[11] Zhao Z, Poyhonen J, Chen Cai X, et al. Augmented reality technology in image-guided therapy: state-of-the-art review. Proc IME H J Eng Med 2021;235:1386–98. https://doi.org/10.1177/09544119211034357.
[12] Badiali G, Cercenelli L, Battaglia S, et al. Review on augmented reality in oral and cranio-maxillofacial surgery: toward "surgery-specific" head-up displays. IEEE Access 2020;8:59015–28. https://doi.org/10.1109/ACCESS.2020.2973298.
[13] Doughty M, Ghugre NR, Wright GA. Augmenting performance: a systematic review of optical see-through head-mounted displays in surgery. J Imaging 2022;8:203. https://doi.org/10.3390/JIMAGING8070203.
[14] Spijkerboer KGP, Fitski M, Siepel FJ, et al. Augmented reality-guided localization of a chest wall tumor in a pediatric patient. Eur J Cancer 2022;170:103–5. https://doi.org/10.1016/j.ejca.2022.04.023.
[15] Fan Y, Jiang D, Wang M, et al. A new markerless patient-to-image registration method using a portable 3D scanner. Med Phys 2014;41:101910. https://doi.org/10.1118/1.4895847.
[16] Dong Y, Zhang C, Ji D, et al. Regional-surface-based registration for image-guided neurosurgery: effects of scan modes on registration accuracy. Int J CARS 2019;14:1303–15. https://doi.org/10.1007/s11548-019-01990-6.
[17] Wu ML, Chien JC, Wu CT, et al. An augmented reality system using improved-iterative closest point algorithm for on-patient medical image visualization. Sensors 2018;18. https://doi.org/10.3390/s18082505.
[18] Xie Y, Zeng R, Yan J, et al. Introducing surface-to-surface matching technique to evaluate mandibular symmetry: a retrospective study. Heliyon 2022;8:e09914. https://doi.org/10.1016/j.heliyon.2022.e09914.
[19] Su ST, Ho MC, Yen JY, et al. Featured surface matching method for liver image registration. IEEE Access 2020;8:59723–31. https://doi.org/10.1109/ACCESS.2020.2983325.
[20] Audette MA, Ferrie FP, Peters TM. An algorithmic overview of surface registration techniques for medical imaging. Med Image Anal 2000;4:201–17. https://doi.org/10.1016/S1361-8415(00)00014-1.
[21] Fedorov A, Beichel R, Kalpathy-Cramer J, et al. 3D slicer as an image computing platform for the quantitative imaging network. Magn Reson Imag 2012;30:1323–41. https://doi.org/10.1016/J.MRI.2012.05.001.
[22] Norrdine A. An algebraic solution to the multilateration problem. In: International Conference on Indoor Positioning and Indoor Navigation; 2015. https://doi.org/10.13140/RG.2.1.1681.3602.
[23] West JB, Fitzpatrick JM, Toms SA, et al. Fiducial point placement and the accuracy of point-based, rigid body registration. Neurosurgery 2001;48:810.
[24] Doughty M, Ghugre NR, Wright GA. Imaging augmenting performance: a systematic review of optical see-through head-mounted displays in surgery. J Imaging 2022;8:203. https://doi.org/10.3390/jimaging8070203. 203 2022;8.
[25] Pratt P, Ives M, Lawton G, et al. Through the HoloLens™ looking glass: augmented reality for extremity reconstruction surgery using 3D vascular models with perforating vessels. Eur Radiol Exp 2018;2:2. https://doi.org/10.1186/s41747-017-0033-2.
[26] Yang R, Li C, Tu P, et al. Development and application of digital maxillofacial surgery system based on mixed reality technology. Front Surgery 2022;8.
[27] Hoch A, Liebmann F, Carrillo F, et al. Augmented reality based surgical navigation of the periacetabular osteotomy of Ganz – a pilot cadaveric study. In: Rauter G, Cattin PC, Zam A, Riener R, Carbone G, Pisla D, editors. New trends in medical and service robotics. Cham: Springer International Publishing; 2021. p. 192–201. https://doi.org/10.1007/978-3-030-58104-6_22.